Robust blind identification of room acoustic channels in symmetric alpha-stable distributed noise environments

Hongsen He, Jing Lu, Jingdong Chen, Xiaojun Qiu, and Jacob Benesty

Citation: The Journal of the Acoustical Society of America **136**, 693 (2014); doi: 10.1121/1.4884760
View online: https://doi.org/10.1121/1.4884760
View Table of Contents: https://asa.scitation.org/toc/jas/136/2
Published by the Acoustical Society of America

Robust blind identification of room acoustic channels in symmetric alpha-stable distributed noise environments

Hongsen He[a)]
Key Laboratory of Modern Acoustics of MOE and Institute of Acoustics, Nanjing University, 22 Hankou Road, Nanjing 210093, China

Jing Lu
Institute of Acoustics and Key Laboratory of Modern Acoustics of MOE, Nanjing University, 22 Hankou Road, Nanjing 210093, China

Jingdong Chen
Northwestern Polytechnical University, 127 Youyi West Road, Xi'an, Shaanxi 710072, China

Xiaojun Qiu
Institute of Acoustics and Key Laboratory of Modern Acoustics of MOE, Nanjing University, 22 Hankou Road, Nanjing 210093, China

Jacob Benesty
INRS-EMT, University of Quebec, 800 de la Gauchetiere Ouest, Suite 6900, Montreal, Quebec H5A 1K6, Canada

(Received 6 July 2013; revised 20 March 2014; accepted 5 June 2014)

Blind multichannel identification is generally sensitive to background noise. Although there have been some efforts in the literature devoted to improving the robustness of blind multichannel identification with respect to noise, most of those works assume that the noise is Gaussian distributed, which is often not valid in real room acoustic environments. This paper deals with the more practical scenario where the noise is not Gaussian. To improve the robustness of blind multichannel identification to non-Gaussian noise, a robust normalized multichannel frequency-domain least-mean M-estimate algorithm is developed. Unlike the traditional approaches that use the squared error as the cost function, the proposed algorithm uses an M-estimator to form the cost function, which is shown to be immune to non-Gaussian noise with a symmetric α-stable distribution. Experiments based on the identification of a single-input/multiple-output acoustic system demonstrate the robustness of the proposed algorithm.
 [http://dx.doi.org/10.1121/1.4884760]

PACS number(s): 43.60.Fg, 43.60.Mn, 43.72.Kb [MAH] Pages: 693–704

I. INTRODUCTION

Blind multichannel identification, which estimates the channel impulse responses of an unknown system based only on the output signals, has the great potential to be used in many applications such as multimedia signal processing (Abed-Meraim *et al.*, 1997), geophysical exploration (Luo and Li, 1998), and communications (Tugnait, 2002) to name a few. As a result, the blind multi-channel identification techniques have drawn a significant amount of research attention in recent years, and many algorithms have been developed, such as the subspace algorithm (Moulines *et al.*, 1995), the least-squares method (Xu *et al.*, 1995), the cross-relation algorithm (Xu *et al.*, 1995; Tong *et al.*, 1994), the two-step maximum likelihood algorithm (Hua, 1996), the higher-order statistics method (Cadzow, 1996), the blind deconvolution approach (Roan *et al.*, 2003), the normalized multichannel frequency-domain least-mean-square (NMCFLMS) algorithm (Huang and Benesty, 2003), etc.

Among those methods, the NMCFLMS algorithm is of particular interest because it employs the fast Fourier transform to identify the impulse responses of a single-input/multiple-output acoustic system in the frequency domain and is, therefore, computationally very efficient. However, this algorithm was found not very robust to additive noise. An improved version of the NMCFLMS algorithm, called robust normalized multichannel frequency-domain least-mean-square (RNMCFLMS), was then developed (Haque and Hasan, 2008); it introduced a constraint on the fullband spectral energy to make it immune to additive Gaussian noise.

However, in many practical environments, noise is generally not Gaussian. For example, in typical teleconferencing applications, there are many different types of acoustic noises such as chair creaks, a keyboard clicking, noise produced from footsteps, a telephone ringing, noise due to pages turning, door slams, and objects dropping (Georgiou *et al.*, 1999). These noise signals are not Gaussian, and the NMCFLMS algorithm and its improved versions often fail

[a)]Author to whom correspondence should be addressed. Also at: School of Information Engineering and Key Laboratory of Special Environment Robot Technology of Sichuan Province, Southwest University of Science and Technology, Mianyang 621010, China. Electronic mail: hongsenhe@gmail.com

to converge in such noise environments. Therefore to make the NMCFLMS-type algorithms robust to non-Gaussian noise has become an important issue.

In this paper, we present a robust normalized multichannel frequency-domain least-mean-M-estimate (RNMCFLMM) algorithm. Unlike the traditional NMCFLMS-type algorithms that use the squared error as the optimization cost function, the presented RNMCFLMM method employs an M-estimate function to form the cost function of the multichannel frequency-domain adaptive filter. Due to the fact that an M-estimator has the ability to deal with outliers picked up by microphones, the resulting algorithm is more robust than the traditional NMCFLMS-type algorithms to non-Gaussian noise with a symmetric α-stable (SαS) distribution. Consequently, the presented RNMCFLMM algorithm is robust to both non-Gaussian and Gaussian noises as it will be justified by experiments.

The rest of this paper is organized as follows. In Sec. II, we formulate the related work and the explicit problem. Section III describes the SαS noise model. In Sec. IV, we first derive the proposed RNMCFLMM algorithm, then select a proper M-estimator and give an adaptive approach to determine the parameters of the M-estimator, and finally analyze the convergence condition of the RNMCFLMM algorithm. Section V experimentally evaluates the robustness of the RNMCFLMM algorithm in non-Gaussian and Gaussian noise environments. Finally, we give our conclusions in Sec. VI.

II. PROBLEM FORMULATION

The input-output relationship, at the discrete-time index n, of a single-input/multiple-output acoustic system is given by

$$x_k(n) = s(n)*h_k + v_k(n), \quad k = 1, 2, \ldots, M, \tag{1}$$

where $s(n)$ is the source signal, h_k is the channel impulse response between the sound source and the kth microphone, which is typically modeled by a finite-impulse-response filter, $v_k(n)$ is the additive noise at the kth microphone, and M is the number of microphones. If we neglect the noise term in Eq. (1), the following relation can be obtained for any two different channels i and j ($i, j = 1, 2, \ldots, M$, and $i \neq j$):

$$\begin{aligned} y_{ij}(n) &= x_i(n) * h_j = s(n)*h_i*h_j \\ &= x_j(n) * h_i \\ &= y_{ji}(n). \end{aligned} \tag{2}$$

This relation can be written in a matrix-vector form as

$$\mathbf{x}_i^T(n)\mathbf{h}_j - \mathbf{x}_j^T(n)\mathbf{h}_i = 0, \tag{3}$$

where

$$\begin{aligned} \mathbf{x}_k(n) &= \left[x_k(n)\ x_k(n-1)\ \cdots\ x_k(n-L+1)\right]^T, \\ & k = 1, 2, \ldots, M, \end{aligned} \tag{4}$$

are the observation signal vectors,

$$\mathbf{h}_k = [h_{k,0}\ h_{k,1}\ \cdots\ h_{k,L-1}]^T, \quad k = 1, 2, \ldots, M, \tag{5}$$

are the impulse response vectors of length L, and $[\cdot]^T$ stands for the transpose of a vector or a matrix.

The cross-relation given in Eq. (3) forms the basis for identifying the M impulse responses. Suppose that $\hat{\mathbf{h}}_k(n)$ is an estimate of $\mathbf{h}_k$ at time n. If $\hat{\mathbf{h}}_k(n)$ deviates from $\mathbf{h}_k$, which is generally true in practice due to several reasons such as the presence of noise, the right-hand side of Eq. (3) is no longer zero, and an *a priori* error signal between the ith and jth channels can be written as

$$\begin{aligned} e_{ij}(n) &= \hat{y}_{ij}(n) - \hat{y}_{ji}(n) \\ &= \mathbf{x}_i^T(n)\hat{\mathbf{h}}_j(n) - \mathbf{x}_j^T(n)\hat{\mathbf{h}}_i(n). \end{aligned} \tag{6}$$

This error signal can then be used to define a cost function that should be minimized to find an optimal estimate of the impulse responses. The NMCFLMS algorithm employs the sum of the squared instantaneous errors between different channels to define the cost function in the frequency-domain (Huang and Benesty, 2003). Using the mth block of the error signal $e_{ij}(n)$, i.e.,

$$\mathbf{e}_{ij}(m) = [e_{ij}(mL)\ e_{ij}(mL+1)\ \cdots\ e_{ij}(mL+L-1)]^T, \tag{7}$$

the cost function of the NMCFLMS algorithm is defined as

$$\mathcal{J}_{\mathrm{F}}(m) = \sum_{i=1}^{M-1}\sum_{j=i+1}^{M} \underline{\boldsymbol{e}}_{ij}^H(m)\underline{\boldsymbol{e}}_{ij}(m), \tag{8}$$

where

$$\begin{aligned} \underline{\boldsymbol{e}}_{ij}(m) &= \mathbf{F}_{L\times L}\mathbf{e}_{ij}(m) \\ &= \boldsymbol{\mathcal{G}}_{L\times 2L}^{01}[\boldsymbol{\mathcal{D}}_{x_i}(m)\boldsymbol{\mathcal{G}}_{2L\times L}^{10}\underline{\hat{\boldsymbol{h}}}_j(m) - \boldsymbol{\mathcal{D}}_{x_j}(m)\boldsymbol{\mathcal{G}}_{2L\times L}^{10}\underline{\hat{\boldsymbol{h}}}_i(m)], \end{aligned} \tag{9}$$

$$\boldsymbol{\mathcal{G}}_{L\times 2L}^{01} = \mathbf{F}_{L\times L}[\mathbf{0}_{L\times L}\ \mathbf{I}_{L\times L}]\mathbf{F}_{2L\times 2L}^{-1}, \tag{10}$$

$$\boldsymbol{\mathcal{D}}_{x_i}(m) = \mathrm{diag}\left[\mathbf{F}_{2L\times 2L}\mathbf{x}_i(m)_{2L\times 1}\right], \tag{11}$$

$$\begin{aligned} \mathbf{x}_i(m)_{2L\times 1} &= [x_i(mL-L) \\ & x_i(mL-L+1)\ \cdots\ x_i(mL+L-1)]^T, \end{aligned} \tag{12}$$

$$\boldsymbol{\mathcal{G}}_{2L\times L}^{10} = \mathbf{F}_{2L\times 2L}[\mathbf{I}_{L\times L}\ \mathbf{0}_{L\times L}]^T\mathbf{F}_{L\times L}^{-1}, \tag{13}$$

$$\underline{\hat{\boldsymbol{h}}}_j(m) = \mathbf{F}_{L\times L}\hat{\mathbf{h}}_j(m), \tag{14}$$

$(\cdot)^H$ denotes the conjugate-transpose of a vector or a matrix, $\mathbf{0}_{L\times L}$ is the null matrix of size $L \times L$, $\mathbf{I}_{L\times L}$ is the identity matrix of size $L \times L$, diag[$\cdot$] denotes a diagonal matrix with the indicated vector along the diagonal or a column vector formed from the main diagonal of a square matrix, $\mathbf{F}_{L\times L}$ and $\mathbf{F}_{L\times L}^{-1}$ are, respectively, the Fourier and inverse Fourier matrices of size $L \times L$, with the (p, q)th element of $\mathbf{F}_{L\times L}$ being

$$(\mathbf{F}_{L\times L})_{p,q} = e^{-\jmath 2\pi(p-1)(q-1)/L}, \quad p, q = 1, 2, \ldots, L, \tag{15}$$

and $\jmath$ is the imaginary unit with $\jmath^2 = -1$. Then the update equations of the NMCFLMS algorithm are derived as

$$\hat{\underline{\boldsymbol{h}}}_k^{10}(m+1) = \hat{\underline{\boldsymbol{h}}}_k^{10}(m) - \mu_{\mathrm{f}} \boldsymbol{\mathcal{P}}_k^{-1}(m) \sum_{i=1}^{M} \boldsymbol{\mathcal{D}}_{x_i}^{*}(m) \underline{\boldsymbol{e}}_{ik}^{01}(m), \quad k = 1, 2, \ldots, M, \tag{16}$$

where μ_{f} is the step size, the superscript * denotes the conjugate operator,

$$\hat{\underline{\boldsymbol{h}}}_k^{10}(m) = \mathbf{F}_{2L\times 2L} \left[\hat{\mathbf{h}}_k^{T}(m) \ \mathbf{0}_{1\times L} \right]^{T}, \tag{17}$$

$$\boldsymbol{\mathcal{P}}_k(m) = \sum_{i=1, i\neq k}^{M} \boldsymbol{\mathcal{D}}_{x_i}^{*}(m) \boldsymbol{\mathcal{D}}_{x_i}(m), \tag{18}$$

$$\underline{\boldsymbol{e}}_{ik}^{01}(m) = \mathbf{F}_{2L\times 2L} \left[\mathbf{0}_{1\times L} \ \mathbf{e}_{ik}^{T}(m) \right]^{T}. \tag{19}$$

The NMCFLMS algorithm can achieve good estimation performance in high signal-to-noise ratio (SNR) environments. The performance of this algorithm, however, deteriorates in low SNR cases. Haque and Hasan proposed an RNMCFLMS algorithm by introducing a constraint on the fullband spectral energy into the NMCFLMS algorithm (Haque and Hasan, 2008). The update equations of the RNMCFLMS algorithm are then formulated as

$$\hat{\underline{\boldsymbol{h}}}_k^{10}(m+1) = \hat{\underline{\boldsymbol{h}}}_k^{10}(m) - \mu_{\mathrm{f}} \nabla \mathcal{J}_{\mathrm{NF},k}^{01}(m) + \mu_{\mathrm{f}} \beta(m) \times \nabla \mathcal{J}_{\mathrm{P},k}^{10}(m), \quad k = 1, 2, \ldots, M, \tag{20}$$

where

$$\nabla \mathcal{J}_{\mathrm{NF},k}^{01}(m) = \boldsymbol{\mathcal{P}}_k^{-1}(m) \sum_{i=1}^{M} \boldsymbol{\mathcal{D}}_{x_i}^{*}(m) \underline{\boldsymbol{e}}_{ik}^{01}(m), \tag{21}$$

$$\nabla \mathcal{J}_{\mathrm{P},k}^{10}(m) = 2\hat{\underline{\boldsymbol{h}}}_k^{10}(m) \oslash |\hat{\underline{\boldsymbol{h}}}_k^{10}(m)|^2, \tag{22}$$

$$\beta(m) = \left| \frac{\left[\nabla \mathcal{J}_{\mathrm{P}}^{10}(m)\right]^{H} \nabla \mathcal{J}_{\mathrm{NF}}^{01}(m)}{\|\nabla \mathcal{J}_{\mathrm{P}}^{10}(m)\|_2^2} \right|, \tag{23}$$

$$\nabla \mathcal{J}_{\mathrm{P}}^{10}(m) = [[\nabla \mathcal{J}_{\mathrm{P},1}^{10}(m)]^{T} \ [\nabla \mathcal{J}_{\mathrm{P},2}^{10}(m)]^{T} \ \cdots \ [\nabla \mathcal{J}_{\mathrm{P},M}^{10}(m)]^{T}]^{T}, \tag{24}$$

$$\nabla \mathcal{J}_{\mathrm{NF}}^{01}(m) = [[\nabla \mathcal{J}_{\mathrm{NF},1}^{01}(m)]^{T} \ [\nabla \mathcal{J}_{\mathrm{NF},2}^{01}(m)]^{T} \ \cdots \ [\nabla \mathcal{J}_{\mathrm{NF},M}^{01}(m)]^{T}]^{T}, \tag{25}$$

$\oslash$ denotes element-by-element division of two vectors, $|\cdot|^2$ is carried out in a component-wise way, and $\|\cdot\|_2$ denotes the ℓ_2 norm. The spectral constraint introduced by the RNMCFLMS algorithm ensures spectral flatness of the estimated channel coefficients in the presence of Gaussian noise (Haque and Hasan, 2008; Haque *et al.*, 2011; Haque *et al.*, 2007). Thus the RNMCFLMS algorithm is robust to Gaussian noise. However, this algorithm is sensitive to non-Gaussian noise. In the following sections, we first model non-Gaussian noise and then propose a robust algorithm for blind identification of a single-input/multiple-output acoustic system.

III. THE SαS NOISE MODEL

A broad and increasingly important class of non-Gaussian phenomena encountered in practice can be characterized as impulsive, such as chair creaks, a keyboard clicking, noise produced from footsteps, a telephone ringing, noise due to pages turning, door slams, and objects dropping (Georgiou *et al.*, 1999). Noises in this class tend to produce large-amplitude excursions from the average value more frequently than Gaussian noise. They are more likely to exhibit sharp spikes or occasional bursts than one would expect from normally distributed noise. Generally, such noise can be modeled by a "zero-centered" SαS distribution (Nikias and Shao, 1995). For noise v with an SαS distribution, its characteristic function is described as

$$\phi(v) = e^{-\gamma |v|^{\alpha}}, \tag{26}$$

where the parameter γ, usually called the dispersion, is a positive constant related to the scale of the distribution, and the shape parameter α $(0 < \alpha \leq 2)$ is called the characteristic exponent. The Gaussian distribution is the limiting case with $\alpha = 2$. The corresponding probability density functions (PDFs) for different values of α are plotted in Fig. 1. It can be seen that a smaller value of α corresponds to a statistical distribution that has a heavier tail. This indicates that there exist more samples far away from the mean or median values; larger bursts (sharp pulses) or more outliers are more likely present in the random process. An important property of the SαS distribution is that only the pth-order $(0 \leq p < \alpha)$ moment exists; this indicates that the second-order statistics (SOS) does not exist if $\alpha < 2$.

IV. THE PROPOSED RNMCFLMM ALGORITHM

A. Algorithm derivation

As mentioned previously, although the RNMCFLMS algorithm is more robust to Gaussian noise, it often fails to converge if the noise is not Gaussian. The underlying reason is that the mean-squared error (MSE)-based criterion can be greatly affected by outliers in the microphone signals, making the resulting algorithm sensitive to non-Gaussian noise (Huber, 1981).

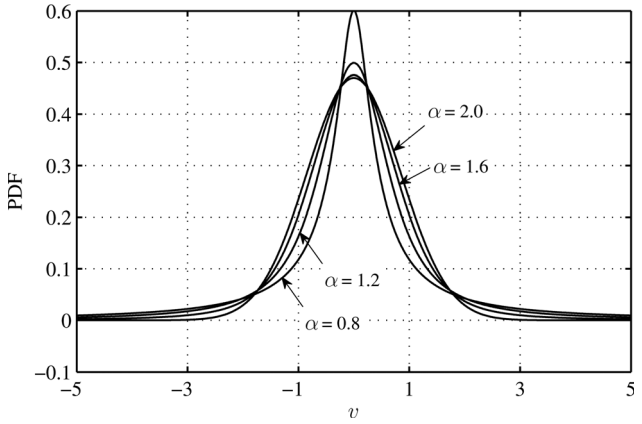

FIG. 1. PDFs of the SαS distribution for different values of α.

This subsection derives the RNMCFLMM algorithm that is more robust than the NMCFLMS-type algorithms to non-Gaussian noise. Instead of using the squared error, we use an M-estimator (Huber, 1981) to form the cost function of the multichannel frequency-domain adaptive filter. The cost function is then defined as

$$\mathcal{J}_{\mathrm{FM}}(m)=\sum_{i=1}^{M-1}\sum_{j=i+1}^{M}\sum_{n=mL}^{mL+L-1}\rho[e_{ij}(n)], \tag{27}$$

where $\rho[\cdot]$ is an M-estimator, which is a real-valued even function, and its first-order derivative is an odd function (more detailed description of the function $\rho[\cdot]$ will be given in Sec. IV B). The comparison between a typical M-estimator and a traditional quadratic function is shown in Fig. 2. It can be seen that when the error signal is small, the M-estimator approaches the quadratic function. However, the M-estimator changes more slowly with the error signal than the quadratic function when the error is large. The purpose of using the M-estimate function, instead of the squared error, is to smooth out the momentary fluctuations due to large bursts, thereby limiting the adverse effect of large bursts on the cost function.

Newton's method (Huang and Benesty, 2003) is used to develop the RNMCFLMM algorithm. To this end, we need to calculate the first-order gradient of $\mathcal{J}_{\mathrm{FM}}(m)$ with respect to $\hat{\underline{\boldsymbol{h}}}_k^*(m)$ and the corresponding Hessian matrix. First of all, we formulate the conjugate of $e_{ij}(n)$ ($n=mL,\ mL+1,\ldots,\ mL+L-1$) as a function of $\hat{\underline{\boldsymbol{h}}}_i^*(m)$ and $\hat{\underline{\boldsymbol{h}}}_j^*(m)$ [notice that $e_{ij}(n)$ is a real number, but we need to do so for calculation], i.e.,

$$\begin{aligned}e_{ij}^*(n)&=\mathbf{e}_{ij}^H(m)\mathbf{u}_{n-mL+1}\\&=\Big[\hat{\underline{\boldsymbol{h}}}_j^H(m)(\boldsymbol{\mathcal{G}}_{2L\times L}^{10})^H\boldsymbol{\mathcal{D}}_{x_i}^H(m)-\hat{\underline{\boldsymbol{h}}}_i^H(m)\\&\quad\times(\boldsymbol{\mathcal{G}}_{2L\times L}^{10})^H\boldsymbol{\mathcal{D}}_{x_j}^H(m)\Big]\mathbf{F}_{2L\times 2L}^{-H}\\&\quad\times\begin{bmatrix}\mathbf{0}_{L\times L} & \mathbf{I}_{L\times L}\end{bmatrix}^H\mathbf{u}_{n-mL+1},\end{aligned} \tag{28}$$

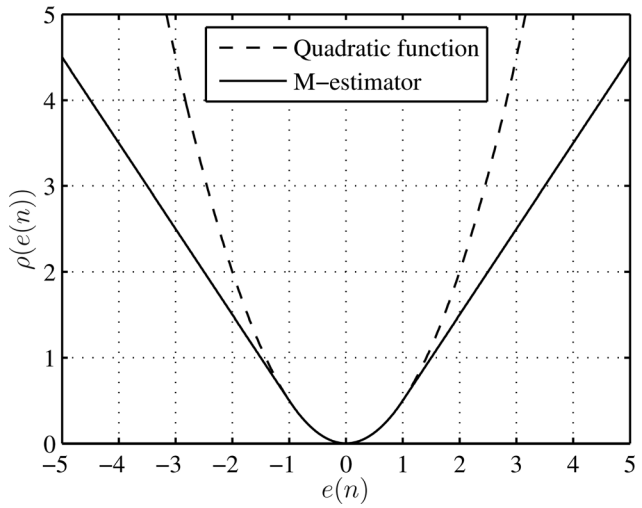

FIG. 2. Comparison between a typical M-estimator and a quadratic function.

where $\mathbf{u}_i$ ($i=1,2,\ldots,L$) is the ith column of the identity matrix $\mathbf{I}_{L\times L}$. Then the derivative of $\sum_{i=1}^{M-1}\sum_{j=i+1}^{M}\rho[e_{ij}(n)]$ with respect to $\hat{\underline{\boldsymbol{h}}}_k^*(m)$ is deduced as

$$\begin{aligned}&\frac{\partial}{\partial\hat{\underline{\boldsymbol{h}}}_k^*(m)}\sum_{i=1}^{M-1}\sum_{j=i+1}^{M}\rho[e_{ij}(n)]\\&=\frac{\partial}{\partial\hat{\underline{\boldsymbol{h}}}_k^*(m)}\left\{\sum_{i=1}^{k-1}\rho[e_{ik}(n)]+\sum_{j=k+1}^{M}\rho[e_{kj}(n)]\right\}\\&=\sum_{i=1}^{k-1}\rho'[e_{ik}(n)]\frac{\partial e_{ik}^*(n)}{\partial\hat{\underline{\boldsymbol{h}}}_k^*(m)}+\sum_{j=k+1}^{M}\rho'[e_{kj}(n)]\frac{\partial e_{kj}^*(n)}{\partial\hat{\underline{\boldsymbol{h}}}_k^*(m)}\\&=\sum_{i=1}^{k-1}\rho'[e_{ik}(n)]\boldsymbol{\mathcal{G}}_{L\times 2L}^{10}\boldsymbol{\mathcal{D}}_{x_i}^*(m)\mathbf{F}_{2L\times 2L}^{-H}\\&\quad\times\begin{bmatrix}\mathbf{0}_{L\times L} & \mathbf{I}_{L\times L}\end{bmatrix}^T\mathbf{u}_{n-mL+1}-\sum_{j=k+1}^{M}\rho'[e_{kj}(n)]\\&\quad\times\boldsymbol{\mathcal{G}}_{L\times 2L}^{10}\boldsymbol{\mathcal{D}}_{x_j}^*(m)\mathbf{F}_{2L\times 2L}^{-H}\begin{bmatrix}\mathbf{0}_{L\times L} & \mathbf{I}_{L\times L}\end{bmatrix}^T\mathbf{u}_{n-mL+1}\\&=\sum_{i=1}^{M}\rho'[e_{ik}(n)]\boldsymbol{\mathcal{G}}_{L\times 2L}^{10}\boldsymbol{\mathcal{D}}_{x_i}^*(m)\mathbf{F}_{2L\times 2L}^{-H}\\&\quad\times\begin{bmatrix}\mathbf{0}_{L\times L} & \mathbf{I}_{L\times L}\end{bmatrix}^T\mathbf{u}_{n-mL+1}\\&=\frac{1}{2L}\sum_{i=1}^{M}\rho'[e_{ik}(n)]\boldsymbol{\mathcal{G}}_{L\times 2L}^{10}\boldsymbol{\mathcal{D}}_{x_i}^*(m)\mathbf{F}_{2L\times 2L}\\&\quad\times\begin{bmatrix}\mathbf{0}_{L\times L} & \mathbf{I}_{L\times L}\end{bmatrix}^T\mathbf{u}_{n-mL+1},\end{aligned} \tag{29}$$

where $\rho'(\cdot)$ is the first-order derivative of $\rho(\cdot)$,

$$\boldsymbol{\mathcal{G}}_{L\times 2L}^{10}=(\boldsymbol{\mathcal{G}}_{2L\times L}^{10})^H=\mathbf{F}_{L\times L}\begin{bmatrix}\mathbf{I}_{L\times L} & \mathbf{0}_{L\times L}\end{bmatrix}\mathbf{F}_{2L\times 2L}^{-1}, \tag{30}$$

and the fourth step follows from the fact $-\rho'[e_{kj}(n)]=\rho'[e_{jk}(n)]$ and $\rho'[e_{kk}(n)]=0$.

Therefore the first-order gradient of $\mathcal{J}_{\mathrm{FM}}(m)$ with respect to $\hat{\underline{\boldsymbol{h}}}_k^*(m)$ is

$$\begin{aligned}\nabla\mathcal{J}_{\mathrm{FM}}(m)&=2\frac{\partial\mathcal{J}_{\mathrm{FM}}(m)}{\partial\hat{\underline{\boldsymbol{h}}}_k^*(m)}\\&=2\sum_{i=1}^{M-1}\sum_{j=i+1}^{M}\sum_{n=mL}^{mL+L-1}\frac{\partial\rho[e_{ij}(n)]}{\partial\hat{\underline{\boldsymbol{h}}}_k^*(m)}\\&=\frac{1}{L}\sum_{i=1}^{M}\sum_{n=mL}^{mL+L-1}\boldsymbol{\mathcal{G}}_{L\times 2L}^{10}\boldsymbol{\mathcal{D}}_{x_i}^*(m)\mathbf{F}_{2L\times 2L}\\&\quad\times\begin{bmatrix}\mathbf{0}_{L\times L} & \mathbf{I}_{L\times L}\end{bmatrix}^T\mathbf{u}_{n-mL+1}\rho'[e_{ik}(n)]\\&=\frac{1}{L}\sum_{i=1}^{M}\boldsymbol{\mathcal{G}}_{L\times 2L}^{10}\boldsymbol{\mathcal{D}}_{x_i}^*(m)\mathbf{F}_{2L\times 2L}\begin{bmatrix}\mathbf{0}_{L\times L} & \mathbf{I}_{L\times L}\end{bmatrix}^T\\&\quad\times\boldsymbol{\varphi}[\mathbf{e}_{ik}(m)],\end{aligned} \tag{31}$$

where

$$\boldsymbol{\varphi}[\mathbf{e}_{ik}(m)]=\begin{bmatrix}\rho'[e_{ik}(mL)]\\\rho'[e_{ik}(mL+1)]\\\vdots\\\rho'[e_{ik}(mL+L-1)]\end{bmatrix}. \tag{32}$$

The Hessian matrix is then derived as follows:

$$\begin{aligned}\boldsymbol{\mathcal{S}}_k(m) &= 2\frac{\partial}{\partial\hat{\underline{\boldsymbol{h}}}_k^*(m)}[\nabla\mathcal{J}_{\mathrm{FM}}(m)]^H \\ &= \frac{2}{L}\frac{\partial}{\partial\hat{\underline{\boldsymbol{h}}}_k^*(m)}\left\{\sum_{i=1,i\neq k}^{M}\boldsymbol{\varphi}^H[\mathbf{e}_{ik}(m)]\right. \\ &\quad\left.\times\begin{bmatrix}\mathbf{0}_{L\times L} & \mathbf{I}_{L\times L}\end{bmatrix}\mathbf{F}_{2L\times 2L}^H\boldsymbol{\mathcal{D}}_{x_i}(m)\boldsymbol{\mathcal{G}}_{2L\times L}^{10}\right\} \\ &= \frac{2}{L}\sum_{i=1,i\neq k}^{M}\frac{\partial\boldsymbol{\varphi}^H[\mathbf{e}_{ik}(m)]}{\partial\hat{\underline{\boldsymbol{h}}}_k^*(m)}\begin{bmatrix}\mathbf{0}_{L\times L} & \mathbf{I}_{L\times L}\end{bmatrix} \\ &\quad\times\mathbf{F}_{2L\times 2L}^H\boldsymbol{\mathcal{D}}_{x_i}(m)\boldsymbol{\mathcal{G}}_{2L\times L}^{10}. \end{aligned} \tag{33}$$

Notice that

$$\begin{aligned}&\frac{\partial\boldsymbol{\varphi}^H[\mathbf{e}_{ik}(m)]}{\partial\hat{\underline{\boldsymbol{h}}}_k^*(m)} \\ &= \left[\rho''[e_{ik}(mL)]\frac{\partial e_{ik}^*(mL)}{\partial\hat{\underline{\boldsymbol{h}}}_k^*(m)} \quad \rho''[e_{ik}(mL+1)]\right. \\ &\quad\times\frac{\partial e_{ik}^*(mL+1)}{\partial\hat{\underline{\boldsymbol{h}}}_k^*(m)}\cdots\rho''[e_{ik}(mL+L-1)] \\ &\quad\left.\times\frac{\partial e_{ik}^*(mL+L-1)}{\partial\hat{\underline{\boldsymbol{h}}}_k^*(m)}\right] \\ &= \left[\rho''[e_{ik}(mL)]\boldsymbol{\mathcal{G}}_{L\times 2L}^{10}\boldsymbol{\mathcal{D}}_{x_i}^*(m)\right. \\ &\quad\times\mathbf{F}_{2L\times 2L}^{-H}\begin{bmatrix}\mathbf{0}_{L\times L} & \mathbf{I}_{L\times L}\end{bmatrix}^T\mathbf{u}_1 \quad \rho''[e_{ik}(mL+1)] \\ &\quad\times\boldsymbol{\mathcal{G}}_{L\times 2L}^{10}\boldsymbol{\mathcal{D}}_{x_i}^*(m)\mathbf{F}_{2L\times 2L}^{-H}\begin{bmatrix}\mathbf{0}_{L\times L} & \mathbf{I}_{L\times L}\end{bmatrix}^T\mathbf{u}_2 \\ &\quad\cdots\rho''[e_{ik}(mL+L-1)]\boldsymbol{\mathcal{G}}_{L\times 2L}^{10}\boldsymbol{\mathcal{D}}_{x_i}^*(m)\mathbf{F}_{2L\times 2L}^{-H} \\ &\quad\left.\times\begin{bmatrix}\mathbf{0}_{L\times L} & \mathbf{I}_{L\times L}\end{bmatrix}^T\mathbf{u}_L\right] \\ &= \boldsymbol{\mathcal{G}}_{L\times 2L}^{10}\boldsymbol{\mathcal{D}}_{x_i}^*(m)\mathbf{F}_{2L\times 2L}^{-H}\begin{bmatrix}\mathbf{0}_{L\times L} & \mathbf{I}_{L\times L}\end{bmatrix}^T\mathbf{T}_{ik}(m), \end{aligned} \tag{34}$$

where

$$\begin{aligned}\mathbf{T}_{ik}(m) = \mathrm{diag}\{&[\rho''[e_{ik}(mL)] \quad \rho''[e_{ik}(mL+1)] \\ &\cdots \quad \rho''[e_{ik}(mL+L-1)]]\}, \end{aligned} \tag{35}$$

$\rho''(\cdot)$ is the second-order derivative of $\rho(\cdot)$, and so by substituting Eq. (34) into Eq. (33) the Hessian matrix is obtained as

$$\boldsymbol{\mathcal{S}}_k(m) = \frac{1}{L}\boldsymbol{\mathcal{G}}_{L\times 2L}^{10}\boldsymbol{\mathcal{P}}_k(m)\boldsymbol{\mathcal{G}}_{2L\times L}^{10}, \tag{36}$$

where

$$\begin{aligned}\boldsymbol{\mathcal{P}}_k(m) =& 2\sum_{i=1,i\neq k}^{M}\boldsymbol{\mathcal{D}}_{x_i}^*(m)\mathbf{F}_{2L\times 2L}^{-H}\begin{bmatrix}\mathbf{0}_{L\times L} & \mathbf{I}_{L\times L}\end{bmatrix}^T \\ &\times\mathbf{T}_{ik}(m)\begin{bmatrix}\mathbf{0}_{L\times L} & \mathbf{I}_{L\times L}\end{bmatrix}\mathbf{F}_{2L\times 2L}^H\boldsymbol{\mathcal{D}}_{x_i}(m). \end{aligned} \tag{37}$$

Using Newton's method, we can write the update equations of the channel estimates as

$$\begin{aligned}\hat{\underline{\boldsymbol{h}}}_k(m+1) = \hat{\underline{\boldsymbol{h}}}_k(m) - \mu\boldsymbol{\mathcal{S}}_k^{-1}(m)\nabla\mathcal{J}_{\mathrm{FM}}(m), \\ k = 1,2,\ldots,M, \end{aligned} \tag{38}$$

where μ is the step size. Substitute Eqs. (31) and (36) into Eq. (38) and pre-multiplying both sides by $\boldsymbol{\mathcal{G}}_{2L\times L}^{10}$, we then obtain the RNMCFLMM algorithm

$$\begin{aligned}&\boldsymbol{\mathcal{G}}_{2L\times L}^{10}\hat{\underline{\boldsymbol{h}}}_k(m+1) \\ &= \boldsymbol{\mathcal{G}}_{2L\times L}^{10}\hat{\underline{\boldsymbol{h}}}_k(m) - \mu\boldsymbol{\mathcal{G}}_{2L\times L}^{10}\left[\boldsymbol{\mathcal{G}}_{L\times 2L}^{10}\boldsymbol{\mathcal{P}}_k(m)\boldsymbol{\mathcal{G}}_{2L\times L}^{10}\right]^{-1} \\ &\quad\times\boldsymbol{\mathcal{G}}_{L\times 2L}^{10}\sum_{i=1}^{M}\boldsymbol{\mathcal{D}}_{x_i}^*(m)\mathbf{F}_{2L\times 2L}[\mathbf{0}_{L\times L}\ \mathbf{I}_{L\times L}]^T \\ &\quad\times\boldsymbol{\varphi}[\mathbf{e}_{ik}(m)], \quad k = 1,2,\ldots,M. \end{aligned} \tag{39}$$

Define the matrix

$$\boldsymbol{\mathcal{G}}_{2L\times 2L}^{10} = \boldsymbol{\mathcal{G}}_{2L\times L}^{10}\boldsymbol{\mathcal{G}}_{L\times 2L}^{10} = \mathbf{F}_{2L\times 2L}\begin{bmatrix}\mathbf{I}_{L\times L} & \mathbf{0}_{L\times L}\\ \mathbf{0}_{L\times L} & \mathbf{0}_{L\times L}\end{bmatrix}\mathbf{F}_{2L\times 2L}^{-1}, \tag{40}$$

and note that

$$\boldsymbol{\mathcal{G}}_{2L\times L}^{10} = \boldsymbol{\mathcal{G}}_{2L\times 2L}^{10}\boldsymbol{\mathcal{G}}_{2L\times L}^{10}, \tag{41}$$

then

$$\boldsymbol{\mathcal{G}}_{2L\times L}^{10}\left[\boldsymbol{\mathcal{G}}_{L\times 2L}^{10}\boldsymbol{\mathcal{P}}_k(m)\boldsymbol{\mathcal{G}}_{2L\times L}^{10}\right]^{-1}\boldsymbol{\mathcal{G}}_{L\times 2L}^{10} = \boldsymbol{\mathcal{G}}_{2L\times 2L}^{10}\boldsymbol{\mathcal{P}}_k^{-1}(m), \tag{42}$$

which can be verified by post-multiplying both sides of Eq. (42) by $\boldsymbol{\mathcal{P}}_k(m)\boldsymbol{\mathcal{G}}_{2L\times L}^{10}$. Now, substituting Eq. (42) into Eq. (39) produces the *constrained* (Haykin, 2002) RNMCFLMM algorithm

$$\begin{aligned}\hat{\underline{\boldsymbol{h}}}_k^{10}(m+1) = \hat{\underline{\boldsymbol{h}}}_k^{10}(m) - \mu\boldsymbol{\mathcal{G}}_{2L\times 2L}^{10}\boldsymbol{\mathcal{P}}_k^{-1}(m) \\ \times\sum_{i=1}^{M}\boldsymbol{\mathcal{D}}_{x_i}^*(m)\underline{\boldsymbol{\varphi}}^{01}[\mathbf{e}_{ik}(m)], \quad k = 1,2,\ldots,M, \end{aligned} \tag{43}$$

where

$$\hat{\underline{\boldsymbol{h}}}_k^{10}(m) = \boldsymbol{\mathcal{G}}_{2L\times L}^{10}\hat{\underline{\boldsymbol{h}}}_k(m), \tag{44}$$

$$\underline{\boldsymbol{\varphi}}^{01}[\mathbf{e}_{ik}(m)] = \mathbf{F}_{2L\times 2L}[\mathbf{0}_{L\times L}\ \mathbf{I}_{L\times L}]^T\boldsymbol{\varphi}[\mathbf{e}_{ik}(m)]. \tag{45}$$

If L is large, $\boldsymbol{\mathcal{G}}_{2L\times 2L}^{10} \approx \mathbf{I}_{2L\times 2L}/2$ (Buchner *et al.*, 2005). Using this approximation, we deduce the *unconstrained* (Haykin, 2002) RNMCFLMM algorithm as

$$\begin{aligned}\hat{\underline{\boldsymbol{h}}}_k^{10}(m+1) = \hat{\underline{\boldsymbol{h}}}_k^{10}(m) - \mu_{\mathrm{f}}\boldsymbol{\mathcal{P}}_k^{-1}(m)\sum_{i=1}^{M}\boldsymbol{\mathcal{D}}_{x_i}^*(m) \\ \times\underline{\boldsymbol{\varphi}}^{01}[\mathbf{e}_{ik}(m)], \quad k = 1,2,\ldots,M, \end{aligned} \tag{46}$$

where the new step size $\mu_{\mathrm{f}} = \mu/2$. To reduce the computational complexity, let us simplify Eq. (35) as

$$\mathbf{T}_{ik}(m) = \rho''[e_{ik}(m)]_{\max}\mathbf{I}_{L\times L}, \tag{47}$$

where

$$\rho''[e_{ik}(m)]_{\max} = \max_{0\le l\le L-1}\{\rho''[e_{ik}(mL+l)]\}. \quad (48)$$

Then using

$$\mathbf{F}_{2L\times 2L}^{-H}[\mathbf{0}_{L\times L}\ \mathbf{I}_{L\times L}]^T\mathbf{T}_{ik}(m)[\mathbf{0}_{L\times L}\ \mathbf{I}_{L\times L}]\ \mathbf{F}_{2L\times 2L}^{H} = \rho''[e_{ik}(m)]_{\max}\mathcal{G}_{2L\times 2L}^{01}, \quad (49)$$

where

$$\mathcal{G}_{2L\times 2L}^{01} = \mathbf{F}_{2L\times 2L}\begin{bmatrix}\mathbf{0}_{L\times L} & \mathbf{0}_{L\times L}\\ \mathbf{0}_{L\times L} & \mathbf{I}_{L\times L}\end{bmatrix}\mathbf{F}_{2L\times 2L}^{-1}, \quad (50)$$

and $\mathcal{G}_{2L\times 2L}^{01} \approx \mathbf{I}_{2L\times 2L}/2$ (Buchner *et al.*, 2005), we can simplify Eq. (37) as

$$\mathcal{P}_k(m) = \sum_{i=1,i\ne k}^{M}\rho''[e_{ik}(m)]_{\max}\mathcal{D}_{x_i}^{*}(m)\mathcal{D}_{x_i}(m). \quad (51)$$

Note that the preceding simplifications may slightly affect the convergence rate and robustness of the algorithm as it is conservative to use only the maximum in Eq. (48). However, it can be seen from Eq. (51) that $\mathcal{P}_k(m)$ is simplified to a diagonal matrix, which largely reduces the computational load of the inversion of $\mathcal{P}_k(m)$.

When there are large bursts present in the microphone signals, the normalization by $\mathcal{P}_k(m)$ in Eq. (51) greatly diminishes the gradient by exploiting the maximum element in $\{\rho''[e_{ik}(mL+l)]\}$, which smoothes out the fluctuation due to large bursts of the microphone signals. Furthermore, unlike the NMCFLMS-type algorithms that are based on the use of $e_{ik}(m)$, the RNMCFLMM algorithm uses $\boldsymbol{\varphi}[\mathbf{e}_{ik}(m)]$, which can limit the adverse effect of large bursts on the update equations when the error signal becomes very large.

To make the proposed algorithm immune to Gaussian noise, we also introduce a similar spectral constraint (Haque and Hasan, 2008; Haque *et al.*, 2011) into the proposed algorithm. So, the update equations of the final RNMCFLMM algorithm are as follows:

$$\hat{\underline{\boldsymbol{h}}}_k^{10}(m+1) = \hat{\underline{\boldsymbol{h}}}_k^{10}(m) - \mu_f\nabla\mathcal{J}_{\mathrm{NFM},k}^{01}(m) + \mu_f\beta(m)\times\nabla\mathcal{J}_{\mathrm{SC},k}^{10}(m),\ \ k=1,2,\ldots,M, \quad (52)$$

where

$$\nabla\mathcal{J}_{\mathrm{NFM},k}^{01}(m) = \mathcal{P}_k^{-1}(m)\sum_{i=1}^{M}\mathcal{D}_{x_i}^{*}(m)\underline{\boldsymbol{\varphi}}^{01}[\mathbf{e}_{ik}(m)], \quad (53)$$

$$\nabla\mathcal{J}_{\mathrm{SC},k}^{10}(m) = 2\hat{\underline{\boldsymbol{h}}}_k^{10}(m)\oslash\left(\mathbf{1}_{2L\times 1} + |\hat{\underline{\boldsymbol{h}}}_k^{10}(m)|^2\right) \quad (54)$$

$\beta(m)$ is the Lagrange multiplier similar to that of the RNMCFLMS algorithm, $\mathbf{1}_{2L\times 1}$, a vector of length $2L$ with all the elements being 1, is introduced to circumvent the mask of the logarithmic calculation [in the penalty function (Haque and Hasan, 2008; Haque *et al.*, 2011)] of some very small elements in $\hat{\underline{\boldsymbol{h}}}_k^{10}(m)$ to that of other elements.

In implementation, the power spectrum of the multiple channel outputs can be obtained by the classical recursive estimate

$$\mathcal{P}_k(m) = \lambda_p\mathcal{P}_k(m-1) + (1-\lambda_p)\times\sum_{i=1,i\ne k}^{M}\rho''[e_{ik}(m)]_{\max}\mathcal{D}_{x_i}^{*}(m)\mathcal{D}_{x_i}(m), \quad (55)$$

where λ_p is a forgetting factor. The recursion in Eq. (55) is equivalent to employing a block-based recursive least M-estimate criterion (Buchner *et al.*, 2006) in Eq. (27). Note that the regularization of $\mathcal{P}_k(m)$ is needed in implementation for numerical stability, and so Eq. (53) is rewritten as

$$\nabla\mathcal{J}_{\mathrm{NFM},k}^{01}(m) = [\mathcal{P}_k(m) + \delta\mathbf{I}_{2L\times 2L}]^{-1}\times\sum_{i=1}^{M}\mathcal{D}_{x_i}^{*}(m)\underline{\boldsymbol{\varphi}}^{01}[\mathbf{e}_{ik}(m)], \quad (56)$$

where δ is a small positive number.

To avoid trivial estimates with all zero elements for the impulse responses, the filter coefficient vectors are normalized to have a unit norm at each update.

B. Choice of the M-estimator

Commonly used M-estimators include the Huber estimator, the Fair estimator, the Geman–McClure estimator, etc. (Zhang, 1997; Wu and Qiu, 2013). For simplicity, the Huber estimator is selected, and then the corresponding estimate function between the ith and jth channels is written as

$$\rho[e_{ij}(n)] = \begin{cases} e_{ij}^2(n)/2, & |e_{ij}(n)| < \xi_{ij}\\ \xi_{ij}[|e_{ij}(n)| - \xi_{ij}/2], & |e_{ij}(n)| \ge \xi_{ij}.\end{cases} \quad (57)$$

If $|e_{ij}(n)| \le \xi_{ij}$, the cost function employs the MSE criterion. However, if $|e_{ij}(n)| \ge \xi_{ij}$, the cost function employs the mean-absolute error (MAE) criterion to deemphasize the effect of outliers, thereby ensuring the convergence of the update equations.

It is seen that the threshold parameter ξ_{ij} plays an important role on the performance of the proposed RNMCFLMM algorithm. This parameter can be estimated by employing the approach in Chan and Zou, (2004) as $\xi_{ij} = 2.576\sigma_{ij}(m)$, where $\sigma_{ij}^2(m)$ is the estimated variance of the mth block of the error signal $e_{ij}(n)$. A robust estimation of $\sigma_{ij}^2(m)$ is given as

$$\sigma_{ij}^2(m) = \lambda_{\sigma_{ij}}\sigma_{ij}^2(m-1) + (1-\lambda_{\sigma_{ij}})c_M\times\mathrm{med}\,[A_{e_{ij}}(m)], \quad (58)$$

where med[·] denotes the median operator, $A_{e_{ij}}(m) = \&\{e_{ij}^2(mL+L-Q), e_{ij}^2(mL+L-Q+1), \ldots, e_{ij}^2(mL+L-1)\}$, Q is the length of the estimation window, $\lambda_{\sigma_{ij}}$ is a forgetting factor, and $c_M = 1.483\,[1 + 5/(Q-1)]$ is a finite sample correction factor. As can be seen, a small Q causes a partial reflection of med$[A_{e_{ij}}(m)]$ on the recent multiple error blocks. A large Q yields a wide reflection of med$[A_{e_{ij}}(m)]$ on the recent multiple error blocks; this results in a smoother med$[A_{e_{ij}}(m)]$; but the use of a large Q increases the use of memory space. Therefore a proper value of Q should be selected in implementation.

C. Convergence analysis of the RNMCFLMM algorithm

In this subsection, we analyze the convergence condition of the RNMCFLMM algorithm. Let us concatenate the M impulse response vectors into a stacked one; then we can write the update equations in Eq. (52) as

$$\underline{\hat{\boldsymbol{h}}}^{10}(m+1)=\underline{\hat{\boldsymbol{h}}}^{10}(m)-\mu_{\mathrm{f}}[\nabla\mathcal{J}_{\mathrm{NFM}}^{01}(m)-\beta(m)\nabla\mathcal{J}_{\mathrm{SC}}^{10}(m)], \tag{59}$$

where

$$\underline{\hat{\boldsymbol{h}}}^{10}(m)=\left[(\underline{\hat{\boldsymbol{h}}}_1^{10}(m))^T\ \ (\underline{\hat{\boldsymbol{h}}}_2^{10}(m))^T\ \ \cdots\ \ (\underline{\hat{\boldsymbol{h}}}_M^{10}(m))^T\right]^T, \tag{60}$$

$$\begin{aligned}\nabla\mathcal{J}_{\mathrm{NFM}}^{01}(m)=\boldsymbol{\mathcal{P}}^{-1}(m)&\left[\left[\sum_{i=1}^{M}\boldsymbol{\mathcal{D}}_{x_i}^{*}(m)\underline{\boldsymbol{\varphi}}^{01}[\mathbf{e}_{i1}(m)]\right]^T\right.\\&\left[\sum_{i=1}^{M}\boldsymbol{\mathcal{D}}_{x_i}^{*}(m)\underline{\boldsymbol{\varphi}}^{01}[\mathbf{e}_{i2}(m)]\right]^T\cdots\\&\left.\left[\sum_{i=1}^{M}\boldsymbol{\mathcal{D}}_{x_i}^{*}(m)\underline{\boldsymbol{\varphi}}^{01}[\mathbf{e}_{iM}(m)]\right]^T\right]^T,\end{aligned} \tag{61}$$

$$\begin{aligned}\boldsymbol{\mathcal{P}}(m)=\mathrm{diag}\{&[\mathrm{diag}\,[\boldsymbol{\mathcal{P}}_1(m)]]^T\ \ [\mathrm{diag}\,[\boldsymbol{\mathcal{P}}_2(m)]]^T\\&\cdots\ [\mathrm{diag}\,[\boldsymbol{\mathcal{P}}_M(m)]]^T\},\end{aligned} \tag{62}$$

$$\begin{aligned}\nabla\mathcal{J}_{\mathrm{SC}}^{10}(m)=[&(\nabla\mathcal{J}_{\mathrm{SC},1}^{10}(m))^T\ \ (\nabla\mathcal{J}_{\mathrm{SC},2}^{10}(m))^T\\&\cdots\ (\nabla\mathcal{J}_{\mathrm{SC},M}^{10}(m))^T]^T.\end{aligned} \tag{63}$$

Now, if we denote $\underline{\boldsymbol{h}}^{10}$ as the true filter in the frequency domain, Eq. (59) can be written as

$$\underline{\boldsymbol{\varepsilon}}^{10}(m+1)=\underline{\boldsymbol{\varepsilon}}^{10}(m)-\mu_{\mathrm{f}}[\nabla\mathcal{J}_{\mathrm{NFM}}^{01}(m)-\beta(m)\nabla\mathcal{J}_{\mathrm{SC}}^{10}(m)], \tag{64}$$

where $\underline{\boldsymbol{\varepsilon}}^{10}(m)=\underline{\hat{\boldsymbol{h}}}^{10}(m)-\underline{\boldsymbol{h}}^{10}$ is the misalignment vector in the frequency domain.

The underlying idea of the RNMCFLMM algorithm is to minimize the cost function from iteration m to iteration $m+1$. In light of this idea, it is reasonable that we analyze the convergence of the RNMCFLMM algorithm based on the mean-square deviation, which is defined as

$$\mathscr{D}(m)=E\left[\|\underline{\boldsymbol{\varepsilon}}^{10}(m)\|_2^2\right], \tag{65}$$

where $E[\cdot]$ denotes mathematical expectation. Taking the squared ℓ_2 norms of both sides of Eq. (64), rearranging terms, and then taking expectations, we obtain

$$\begin{aligned}&\mathscr{D}(m+1)-\mathscr{D}(m)\\&=\mu_{\mathrm{f}}^2E\left[\|\nabla\mathcal{J}_{\mathrm{NFM}}^{01}(m)-\beta(m)\nabla\mathcal{J}_{\mathrm{SC}}^{10}(m)\|_2^2\right]\\&\quad-2\mu_{\mathrm{f}}E\left\{\mathrm{Re}\left[(\underline{\boldsymbol{\varepsilon}}^{10}(m))^H(\nabla\mathcal{J}_{\mathrm{NFM}}^{01}(m)\right.\right.\\&\quad\left.\left.-\beta(m)\nabla\mathcal{J}_{\mathrm{SC}}^{10}(m))\right]\right\},\end{aligned} \tag{66}$$

where $\mathrm{Re}(\cdot)$ stands for the real part of a complex number. It is obvious that the RNMCFLMM algorithm is convergent in the MSE sense only if $\mathscr{D}(m+1)-\mathscr{D}(m)$ is negative. Therefore we obtain the upper bound of the step-size parameter μ_{f} as

$$\frac{2E\left\{\mathrm{Re}\left[(\underline{\boldsymbol{\varepsilon}}^{10}(m))^H(\nabla\mathcal{J}_{\mathrm{NFM}}^{01}(m)-\beta(m)\nabla\mathcal{J}_{\mathrm{SC}}^{10}(m))\right]\right\}}{E\left[\|\nabla\mathcal{J}_{\mathrm{NFM}}^{01}(m)-\beta(m)\nabla\mathcal{J}_{\mathrm{SC}}^{10}(m)\|_2^2\right]}. \tag{67}$$

V. SIMULATIONS

This section investigates the robustness of the proposed RNMCFLMM algorithm in Eq. (52) to both non-Gaussian and Gaussian noises in acoustic environments. We also compare the RNMCFLMM algorithm with the original NMCFLMS and RNMCFLMS algorithms in different noisy environments to demonstrate the superiority of the proposed algorithm.

As to the aforementioned three algorithms, the initialization of the modeling filter coefficients is similar to Huang and Benesty (2003), the step size μ_{f} is set to 0.5 unless otherwise specified, $\lambda_p=[1-1/(3L)]^L$, the regularization factor δ is initially set to one-fifth of the total power over all channels at the first block. For the proposed RNMCFLMM algorithm, $\lambda_{\sigma_{ij}}, i,j=1,2,\ldots,M$, are set to 0.95, $\sigma_{ij}^2(0)=0$, the length of the estimation window Q is set to $10L$ unless otherwise stated.

A. Experimental environment

The channel impulse responses used in this paper were measured in the Varechoic chamber at Bell Labs (Härmä, 2001). The dimension of the chamber is 6.7 m × 6.1 m × 2.9 m. For convenience, positions in the room are designated by (x, y, z) coordinates with reference to the northwest corner of the chamber floor. An equispaced linear array that consists of three omnidirectional microphones is employed in the measurement, and the spacing between adjacent microphones is 0.7 m. The three microphones of the array are situated at (2.337, 0.500, 1.400), (3.037, 0.500, 1.400), and (3.737, 0.500, 1.400), respectively. A sound source (a loudspeaker) is placed at (0.337, 3.938, 1.600). The impulse responses of the acoustic channels between the source and microphones were measured at a 48 kHz sampling rate when 89% panels on the walls were open and the corresponding reverberation time T_{60} of the chamber was about 280 ms (Härmä, 2001). Then the obtained channel impulse responses are downsampled to a 16 kHz sampling rate and truncated to 256 samples (the zeros shared by all the impulse responses at the beginning are removed). The measured impulse responses will be treated as the actual impulse responses in the experiments.

The sound source signals are white Gaussian noise and a speech signal (from a female English speaker) sampled at 16 kHz, respectively, which have the same sample length of 1.5015×10^6. The multichannel system outputs are computed by convolving the sound source signal with the corresponding measured channel impulse responses and adding

synthetic noise to the results at a given pseudo-SNR (PSNR) [note that the variance of the noise does not exist when $\alpha < 2$; so we use the PSNR to measure the noise level for finite sample realizations (Tsakalides and Nikias, 1995)]. The noise is modeled by the SαS distribution in Sec. III in which the parameter α controls the amount of the sharp pulses in the noise. We employ an effective method presented in Nikias and Shao (1995) and Chambers *et al.* (1976) to simulate the non-Gaussian noise. This method involves a nonlinear transformation of two independent uniform random variables into one stable random variable. This stable random variable is a continuous function of each of the uniform random variables and of α and a modified skewness parameter throughout their respective permissible ranges. Figure 3 depicts the non-Gaussian noises for different values of α.

B. Performance criterion

Different from non-blind channel identification methods, blind single-input/multiple-output identification algorithms determine the channel impulse responses up to a scale. As a result, the normalized projection misalignment (NPM) (Morgan *et al.*, 1998) is extensively used as a performance measure for assessing a blind single-input/multiple-output identification. So we also adopt the NPM as the criterion to evaluate the performance improvement of blind channel identification algorithms in this paper. The NPM at block m is defined as

$$\mathrm{NPM}(m) = 20\log_{10}\left[\frac{\|\boldsymbol{\epsilon}(m)\|_2}{\|\mathbf{h}\|_2}\right] \mathrm{dB}, \tag{68}$$

where

$$\mathbf{h} = [\mathbf{h}_1^T \ \mathbf{h}_2^T \ \cdots \ \mathbf{h}_M^T]^T \tag{69}$$

consists of the true impulse responses,

$$\boldsymbol{\epsilon}(m) = \mathbf{h} - \frac{\mathbf{h}^T\hat{\mathbf{h}}(m)}{\hat{\mathbf{h}}^T(m)\hat{\mathbf{h}}(m)}\hat{\mathbf{h}}(m) \tag{70}$$

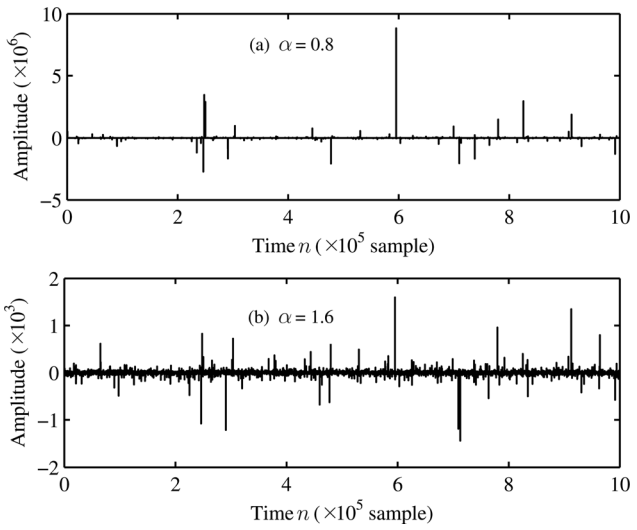

FIG. 3. Non-Gaussian noises for different values of α.

is the projection misalignment vector, $\hat{\mathbf{h}}(m)$ is defined in a similar way to Eq. (69); but it consists of the estimates of the impulse responses. In the following experiments, all the plotted results are obtained by averaging over 100 runs.

C. Experimental results

Figure 4 plots the convergence performance of the NMCFLMS, RNMCFLMS, and proposed RNMCFLMM algorithms for the identification of a three-channel acoustic system (which is excited by a white Gaussian noise) in SαS noise where $L = 256$, $\mathrm{PSNR} = 15\,\mathrm{dB}$, and $\alpha = 1.2$. It is observed that the NMCFLMS and RNMCFLMS algorithms diverge due to the SOS-based cost function, while the proposed RNMCFLMM algorithm converge because the M-estimator can deal with outliers in microphone signals. It is clear that the proposed algorithm is robust to non-Gaussian noise.

Figure 5 plots the convergence performance of the NMCFLMS, RNMCFLMS, and RNMCFLMM algorithms for the identification of a three-channel acoustic system in white Gaussian noise where $L = 256$, $\mathrm{PSNR} = 15\,\mathrm{dB}$, and $\alpha = 2.0$. The system is again excited by a white Gaussian noise. It is seen that the NMCFLMS algorithm is not robust to Gaussian noise. The RNMCFLMS algorithm outperforms the NMCFLMS algorithm in the Gaussian noise environment because a spectral energy constraint is introduced by the former to ensure spectral flatness of the estimated channel coefficients (Haque and Hasan, 2008; Haque *et al.*, 2007). The proposed RNMCFLMM algorithm outperforms the other two, achieving a good compromise between convergence rate and low estimation variance. Due to the dynamic change of the threshold ξ_{ij} of the M-estimator, it is possible that the error signal $|e_{ij}(n)| \geq \xi_{ij}$ even under Gaussian noise conditions. So, the M-estimator alternately employs the MAE and MSE criteria as shown in Fig. 6, such that the proposed RNMCFLMM algorithm obtains the smaller steady-state error but at the cost of a slower

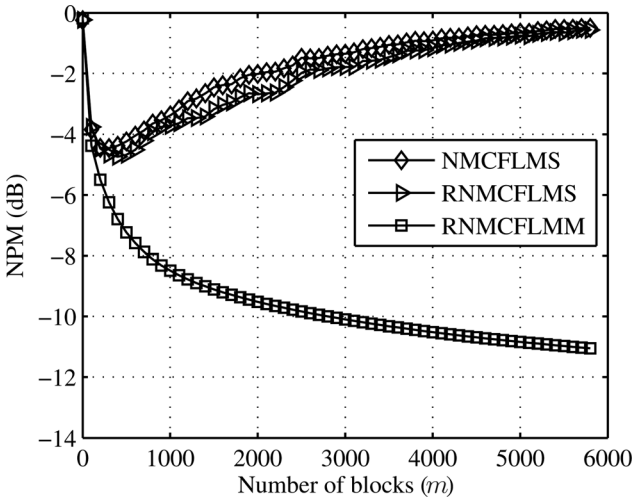

FIG. 4. Convergence of the NMCFLMS, RNMCFLMS, and proposed RNMCFLMM algorithms for the identification of a three-channel acoustic system in SαS noise where $L = 256$, $\mathrm{PSNR} = 15\,\mathrm{dB}$, and $\alpha = 1.2$. The system is excited by a white Gaussian noise.

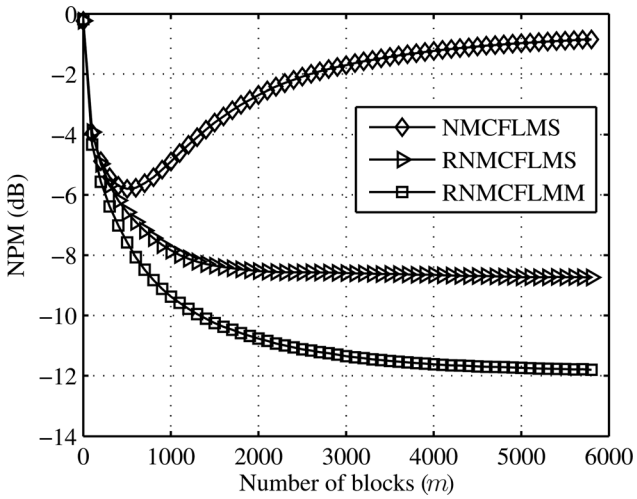

FIG. 5. Convergence of the NMCFLMS, RNMCFLMS, and proposed RNMCFLMM algorithms for the identification of a three-channel acoustic system in white Gaussian noise where $L = 256$, PSNR = 15 dB, and $\alpha = 2.0$. The system is excited by a white Gaussian noise.

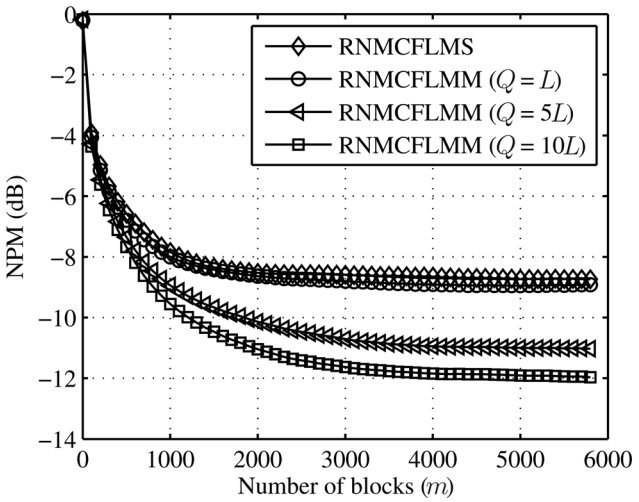

FIG. 7. Effect of the M-estimator on the performance of the proposed RNMCFLMM algorithm for the acoustic channel identification of a three-channel acoustic system in white Gaussian noise where $L = 256$, PSNR = 15 dB, and $\alpha = 2.0$. The system is excited by a white Gaussian noise.

convergence rate. Note that in the implementation, the estimate of $\rho[e_{ij}(n)]$ is smoother than $e_{ij}(n)$ in RNMCFLMS because several blocks of data are used to estimate ξ_{ij} in the M-estimator. This can also reduce the steady-state error of the proposed RNMCFLMM algorithm as shown in Fig. 7.

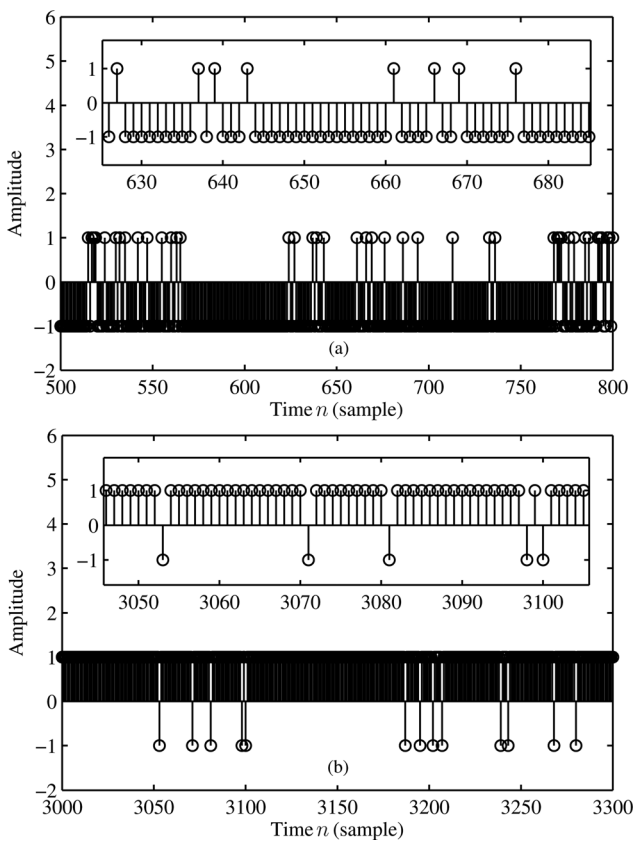

FIG. 6. The alternative operation of the M-estimator corresponding to channels 1 and 2 between the MSE and MAE criteria when considering a segment of adaptive iteration for once implementation [(a): n from 500 to 800, (b): n from 3000 to 3300], where the amplitude of 1 denotes that the MSE criterion works while the amplitude of -1 implies that the MAE criterion does. The parameters are: $L = 256$, PSNR = 15 dB, and $\alpha = 2.0$. The system is excited by a white Gaussian noise.

In this experiment, we compare the NMCFLMS, RNMCFLMS, and RNMCFLMM algorithms for their performance in different PSNR conditions. Again, we consider the same three-channel acoustic system studied in the previous experiments. The system is excited by a white Gaussian noise. Figure 8 depicts the NPM of the three studied algorithms as a function of PSNR in different types of noise environments. It can be seen from Fig. 8 that the NMCFLMS algorithm is sensitive to both non-Gaussian and Gaussian noises. Although the RNMCFLMS algorithm is more robust to Gaussian noise than the NMCFLMS method, this algorithm is seen sensitive to non-Gaussian noise. The proposed RNMCFLMM algorithm is robust to both non-Gaussian and Gaussian noises in all the different PSNR conditions.

In the fourth experiment, we investigate the scenario where the system is excited by speech. The experimental configuration is the same as the previous experiments except that now the excitation is a speech signal instead of a white Gaussian noise. The PSNR is 15 dB. Figures 9 and 10 plot the convergence performance of the NMCFLMS, RNMCFLMS, and RNMCFLMM algorithms in both SαS ($\alpha = 1.2$) and Gaussian ($\alpha = 2.0$) noises, respectively. It is observed that the non-stationarity of speech degrades the performance of all the algorithms as compared to the case with white noise excitation. It is seen that the proposed RNMCFLMM algorithm exhibits the best performance regardless of whether the noise is Gaussian or non-Gaussian, which, again, demonstrates the good performance of this new algorithm.

In the fifth experiment, we compare the NMCFLMS, RNMCFLMS, and RNMCFLMM algorithms for their performance in different PSNR conditions when the system is excited by a speech signal. Figure 11 depicts the NPM of the three algorithms as a function of the PSNR in four different types of noise. Similar to what was observed in Fig. 8, one can see that the RNMCFLMS method is more robust to white Gaussian noise than the original NMCFLMS

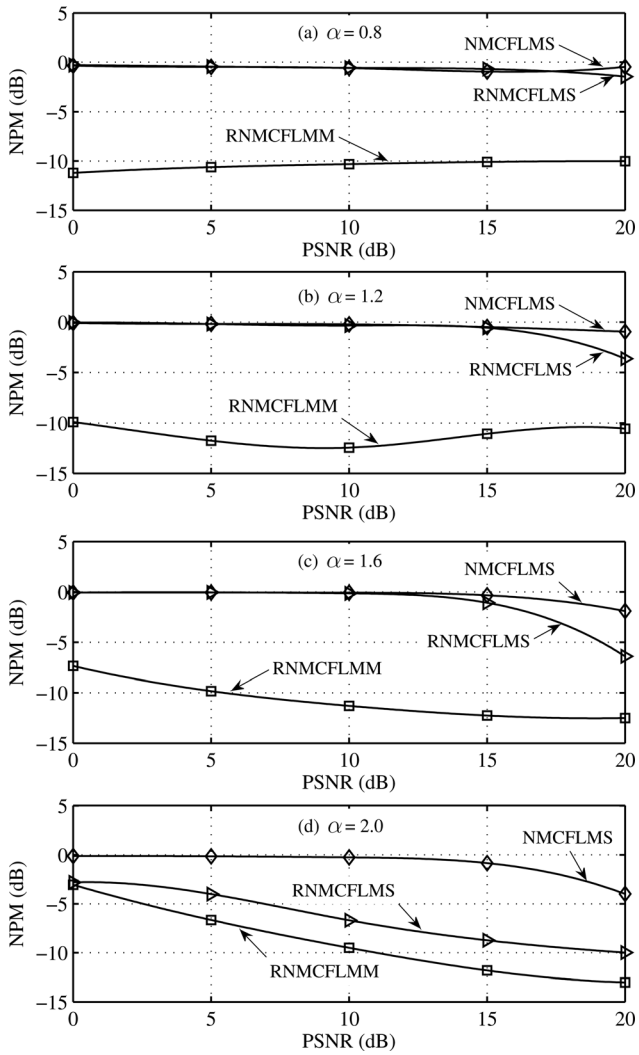

FIG. 8. NPM of the NMCFLMS, RNMCFLMS, and proposed RNMCFLMM algorithms versus PSNR for the identification of a three-channel acoustic system ($L = 256$) in four different types of noises where $\alpha = 0.8, 1.2, 1.6, 2.0$. The system is excited by a white Gaussian noise.

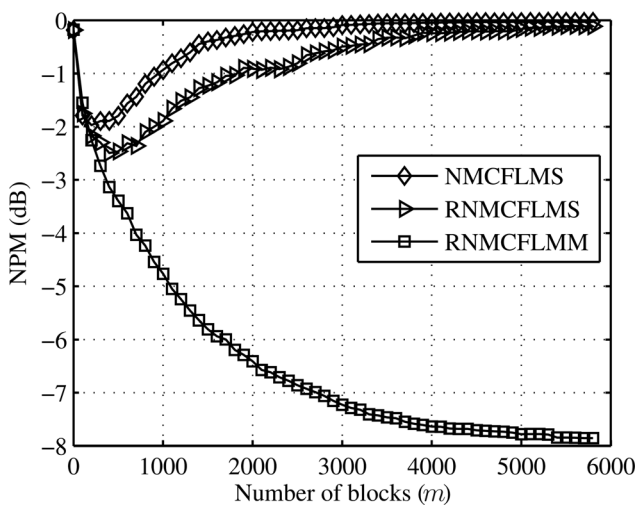

FIG. 9. Convergence of the NMCFLMS, RNMCFLMS, and proposed RNMCFLMM algorithms for the identification of a three-channel acoustic system in SαS noise where $L = 256$, PSNR = 15 dB, and $\alpha = 1.2$. The system is excited by speech.

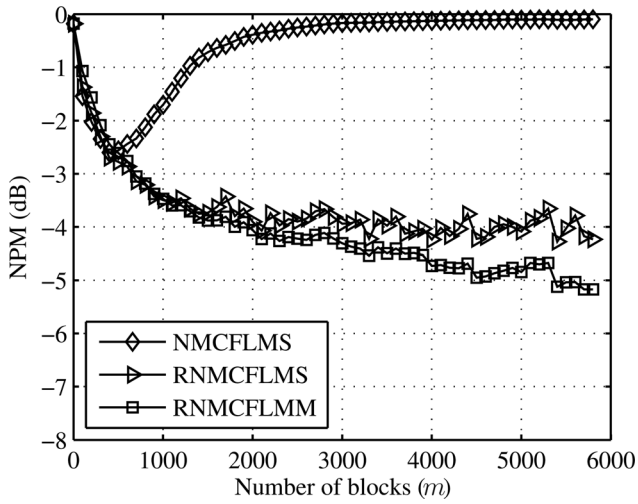

FIG. 10. Convergence of the NMCFLMS, RNMCFLMS, and proposed RNMCFLMM algorithms for the identification of a three-channel acoustic system in white Gaussian noise where $L = 256$, PSNR = 15 dB, and $\alpha = 2.0$. The system is excited by speech.

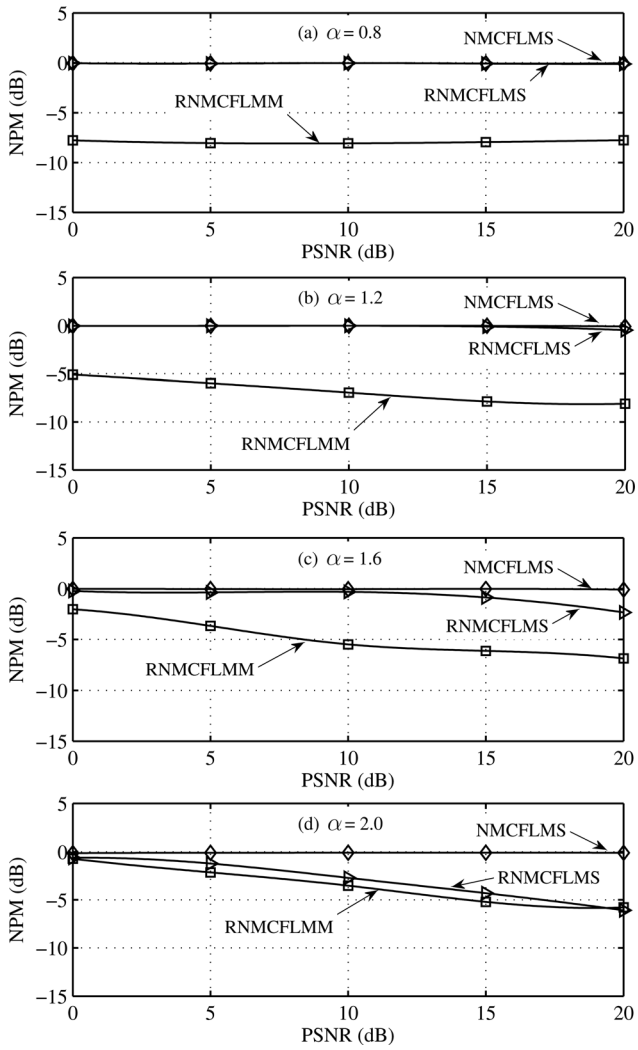

FIG. 11. NPM of the NMCFLMS, RNMCFLMS, and proposed RNMCFLMM algorithms versus PSNR for the identification of a three-channel acoustic system ($L = 256$) in SαS and Gaussian noise conditions where $\alpha = 0.8, 1.2, 1.6, 2.0$. The system is excited by speech.

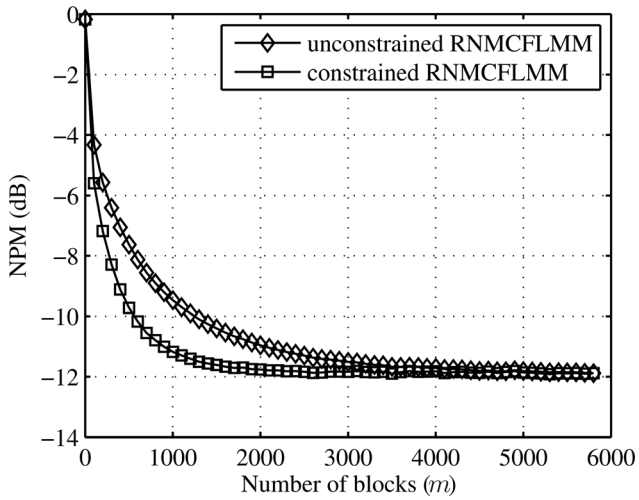

FIG. 12. Convergence of the constrained and unconstrained versions of the proposed RNMCFLMM algorithm for the identification of a three-channel acoustic system in white Gaussian noise where $L = 256$, PSNR = 15 dB, and $\alpha = 2.0$. The system is excited by a white Gaussian noise.

algorithm. But these two algorithms have similar performance when the noise is not Gaussian. In comparison, the proposed RNMCFLMM algorithm yields the best performance in both Gaussian and non-Gaussian noises.

The previous experiments investigate the performance of the unconstrained RNMCFLMM algorithm as a result of Eq. (46). In this experiment, we compare the constrained with unconstrained versions (Haykin, 2002) of the proposed RNMCFLMM algorithm where the system is excited by white noise with the PSNR of 15 dB. Figures 12 and 13 illustrate the convergence performance of the two versions of the RNMCFLMM algorithm in both Gaussian ($\alpha = 2.0$) and non-Gaussian ($\alpha = 1.2$) noises, respectively. It is seen from Fig. 12 that in the Gaussian noise environment, the constrained version has faster convergence rate than the unconstrained one, and the latter needs about twice more iterations than the former to achieve the same NPM, which is consistent with the classical frequency-domain adaptive filter theory (Haykin, 2002; Lee and Un, 1989). Comparing Figs. 12 and 13, one can see that the difference between the convergence rates of the constrained and unconstrained versions of the RNMCFLMM algorithm is similar in the non-Gaussian and Gaussian noises. Please note that in the non-Gaussian noise case, the step size μ_f is set to 1.2 to converge fast.

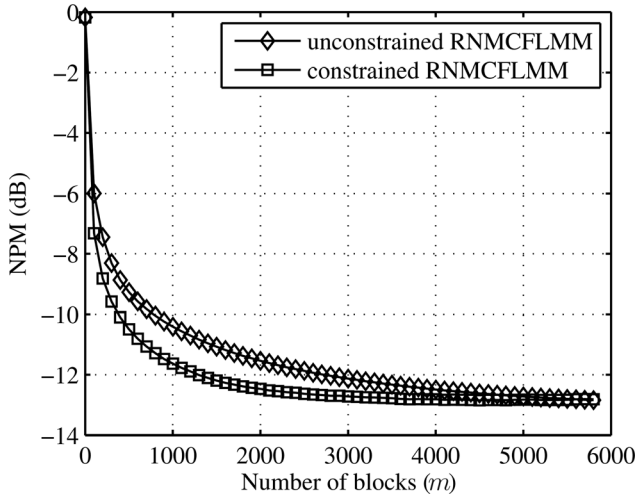

FIG. 13. Convergence of the constrained and unconstrained versions of the proposed RNMCFLMM algorithm for the identification of a three-channel acoustic system in SαS noise where $L = 256$, PSNR = 15 dB, $\alpha = 1.2$, and $\mu_f = 1.2$. The system is excited by a white Gaussian noise.

VI. CONCLUSIONS

In this paper, an adaptive RNMCFLMM algorithm is developed to blindly identify the impulse responses of a single-input/multiple-output acoustic system, which is interfered by SαS non-Gaussian and Gaussian noises. The RNMCFLMM algorithm employs an M-estimator to construct the cost function of the multichannel frequency-domain adaptive filter. The ability of the M-estimator to discriminate outliers of ouput signals help improve the robustness of the RNMCFLMM algorithm to non-Gaussian noise. Experiments were performed to identity a single-input/multiple-output acoustic system in different noise environments. The results demonstrated that the proposed RNMCFLMM algorithm is robust to noise in different PSNR conditions regardless of whether the noise is Gaussian and non-Gaussian.

ACKNOWLEDGMENTS

The effort of the first author is supported by the Incubation Program for the Distinguished Youth Foundation of Sichuan Province of China (Grant No. 2014JQ0042), the Doctoral Foundation of Southwest University of Science and Technology (Grant No. 13zx7149), and the Open Foundation of the Key Laboratory of Modern Acoustics of Nanjing University (Grant No. 1302). The effort of the second author is partially supported by the NSFC (Grant No. 11374156).

Abed-Meraim, K., Qiu, W., and Hua, Y. (**1997**). "Blind system identification," Proc. IEEE **85**, 1310–1322.
Buchner, H., Benesty, J., Gänsler, T., and Kellermann, W. (**2006**). "Robust extended multidelay filter and double-talk detector for acoustic echo cancellation," IEEE Trans. Audio, Speech, Lang. Process. **14**, 1633–1644.
Buchner, H., Benesty, J., and Kellermann, W. (**2005**). "Generalized multichannel frequency- domain adaptive filtering: Efficient realization and application to hands-free speech communication," Elsevier Signal Process. **85**, 549–570.
Cadzow, J. A. (**1996**). "Blind deconvolution via cumulant extrema," IEEE Signal Process. Mag. **13**, 24–42.
Chambers, J. M., Mallows, C. L., and Stuck, B. W. (**1976**). "A method for simulating stable random variables," J. Am. Statist. Assoc. **71**, 340–344.
Chan, S. C., and Zou, Y. X. (**2004**). "A recursive least M-estimate algorithm for robust adaptive filtering in impulse noise: Fast algorithm and convergence performance analysis," IEEE Trans. Signal Process. **52**, 975–991.
Georgiou, P. G., Tsakalides, P., and Kyriakakis, C. (**1999**). "Alpha-stable modeling of noise and robust time-delay estimation in the presence of impulsive noise," IEEE Trans. Multimedia **1**, 291–301.
Haykin, S. (**2002**). *Adaptive Filter Theory*, 4th ed. (Prentice Hall, Englewood Cliffs, NJ), pp. 1–777.
Haque, M. A., Bashar, M., Naylor, P., Hirose, K., and Hasan, M. K. (**2007**). "Energy constrained frequency-domain normalized LMS algorithm for blind channel identificatio," J. Signal, Image Video Process. **1**, 203–213.

Haque, M. A., and Hasan, M. K. (**2008**). "Noise robust multichannel frequency-domain LMS algorithms for blind channel identification," IEEE Signal Process. Lett. **15**, 305–308.
Haque, M. A., Islam, T., and Hasan, M. K. (**2011**). "Robust speech dereverberation based on blind adaptive estimation of acoustic channels," IEEE Trans. Audio, Speech, Lang. Process. **19**, 775–787.
Härmä, A. (**2001**). "Acoustic measurement data from the varechoic chamber," *Technical Memo. No. 110101* (Agere Systems, Allentown, PA).
Hua, Y. (**1996**). "Fast maximum likelihood for blind identification of multiple FIR channels," IEEE Trans. Signal Process. **44**, 661–672.
Huang, Y., and Benesty, J. (**2003**). "A class of frequency-domain adaptive approaches to blind multichannel identification," IEEE Trans. Signal Process. **51**, 11–24.
Huber, P. J. (**1981**). *Robust Statistics* (Wiley, New York), pp. 1–308.
Lee, J. C., and Un, C. K. (**1989**). "Performance analysis of frequency-domain block LMS adaptive digital filters," IEEE Trans. Circuits Syst. **36**, 173–189.
Luo, H., and Li, Y. (**1998**). "The application of blind channel identification techniques to prestack seismic deconvolution," Proc. IEEE **86**, 2082–2089.
Morgan, D. R., Benesty, J., and Sondhi, M. M. (**1998**). "On the evaluation of estimated impulse responses," IEEE Signal Process. Lett. **5**, 174–176.
Moulines, E., Duhamel, P., Cardoso, J. F., and Mayrargue, S. (**1995**). "Subspace methods for the blind identification of multichannel FIR filters," IEEE Trans. Signal Process. **43**, 516–525.
Nikias, C. L., and Shao, M. (**1995**). *Signal Processing with Alpha-Stable Distributions and Applications* (Wiley, New York), pp. 1–168.
Roan, M. J., Gramann, M. R., Erling, J. G., and Sibul, L. H. (**2003**). "Blind deconvolution applied to acoustical systems identification with supporting experimental results," J. Acoust. Soc. Am. **114**, 1988–1996.
Tong, L., Xu, G., and Kailath, T. (**1994**). "Blind identification and equalization based on second- order statistics: A time domain approach" IEEE Trans. Inf. Theory **40**, 340–349.
Tsakalides, P., and Nikias, C. L. (**1995**). "Maximum likelihood localization of sources in noise modeled as a stable process," IEEE Trans. Signal Process. **43**, 2700–2713.
Tugnait, J. K. (**2002**). "A multidelay whitening approach to blind identification and equalization of SIMO channels," IEEE Trans. Wireless Commun. **1**, 456–467.
Wu, L., and Qiu, X. (**2013**). "An M-estimator based algorithm for active impulse-like noise control," Elsevier Appl. Acoust. **74**, 407–412.
Xu, G., Liu, H., Tong, L., and Kailath, T. (**1995**). "A least-squares approach to blind channel identification," IEEE Trans. Signal Process. **43**, 2982–2993.
Zhang, Z. (**1997**). "Parameter estimation techniques: A tutorial with application on conic fitting," Image Vis. Comput. **15**, 59–76.